

Influence of charge compensation mechanisms on the sheet electron density at conducting LaAlO₃/SrTiO₃-interfaces

F. Gunkel, P. Brinks, S. Hoffmann-Eifert, R. Dittmann, M. Huijben et al.

Citation: [Appl. Phys. Lett.](#) **100**, 052103 (2012); doi: 10.1063/1.3679139

View online: <http://dx.doi.org/10.1063/1.3679139>

View Table of Contents: <http://apl.aip.org/resource/1/APPLAB/v100/i5>

Published by the [American Institute of Physics](#).

Additional information on Appl. Phys. Lett.

Journal Homepage: <http://apl.aip.org/>

Journal Information: http://apl.aip.org/about/about_the_journal

Top downloads: http://apl.aip.org/features/most_downloaded

Information for Authors: <http://apl.aip.org/authors>

ADVERTISEMENT

The advertisement banner features a background of orange and yellow diagonal stripes. On the left, there is a white icon of an envelope. To its right, the text 'AIP | Applied Physics Letters' is written in white. Below this, a yellow box contains the text 'Accepting Submissions in Biophysics and Bio-Inspired Systems'. To the right of this box is a white button with the text 'Submit Today' in orange. On the far right, there is a logo for 'AIP Publishing' in blue and yellow.

Influence of charge compensation mechanisms on the sheet electron density at conducting LaAlO₃/SrTiO₃-interfaces

F. Gunkel,^{1,a)} P. Brinks,² S. Hoffmann-Eifert,¹ R. Dittmann,¹ M. Huijben,² J. E. Kleibeuker,² G. Koster,² G. Rijnders,² and R. Waser¹

¹Peter Gruenberg Institut and JARA-FIT, Forschungszentrum Juelich, 52425 Juelich, Germany

²Faculty of Science and Technology, MESA+ Institute for Nanotechnology, University of Twente, P.O. Box 217, 7500 AE Enschede, The Netherlands

(Received 10 August 2011; accepted 5 January 2012; published online 30 January 2012)

The equilibrium conductance of LaAlO₃/SrTiO₃ (LAO/STO)-heterointerfaces was investigated at high temperatures (950 K–1100 K) as a function of ambient oxygen partial pressure (p_{O_2}). Metallic LAO/STO-interfaces were obtained for LAO grown on STO single crystals as well as on STO-buffered (La,Sr)(Al,Ta)O₃ substrates. For both structures, the high temperature sheet carrier density n_s of the LAO/STO-interface saturates at a value of about $1 \times 10^{14} \text{ cm}^{-2}$ for reducing conditions, which indicates the presence of interfacial donor states. A significant decrease of n_s is observed at high oxygen partial pressures. According to the defect chemistry model of donor-doped STO, this behavior for oxidizing conditions can be attributed to the formation of Sr-vacancies as charge compensating defects. © 2012 American Institute of Physics. [doi:10.1063/1.3679139]

The metallic conductivity of the heteroepitaxial interface between LaAlO₃ (LAO) and SrTiO₃ (STO) has generated enormous scientific interest.¹ The underlying physical mechanisms, however, are still under controversial debate.^{2–4} In particular, the impact of crystal disorder and defects on the electrical properties of the LAO/STO-interface has become the central aspect of the ongoing discussion. In this context, lanthanum ions on strontium sites ($\text{La}_{\text{Sr}}^{\bullet}$)^{5–10} and oxygen vacancies ($\text{V}_{\text{O}}^{\bullet\bullet}$) within the STO substrate^{11–15} have been proposed as predominant defects at the LAO/STO-interface since both types of defects can cause n -type conductivity in STO. High temperature equilibrium measurements show an oxygen partial pressure (p_{O_2}) independent interface conductance in a certain p_{O_2} regime.⁶ This supports the model of immobile donors and excludes mobile $\text{V}_{\text{O}}^{\bullet\bullet}$ as origin of the electronic charge carriers. However, the charge compensation mechanism in donor-doped STO is more complex than in conventional semiconductor materials. Intrinsic acceptor-like defects such as Sr-vacancies (V_{Sr}'') can form in STO and act as electron traps (ionic compensation).¹⁶ Thus, an increased amount of V_{Sr}'' will result in a decrease of the electron density, and at the extreme, in a change from n -type metallic to insulating behavior. In previous studies, the conductivity of the LAO/STO-interface has been related to the formation of donor-type defects, i.e., $\text{V}_{\text{O}}^{\bullet\bullet}$ and $\text{La}_{\text{Sr}}^{\bullet}$. However, an additional, complementary influence of acceptor-type defects has not been considered so far.

This aspect will be addressed in the present study which investigates the high temperature equilibrium conductance (HTEC) of two types of LAO/STO-interfaces *in situ* as a function of ambient oxygen partial pressure ($10^{-23} \text{ bar} < p_{\text{O}_2} < 10^{-2} \text{ bar}$) in the temperature range from 950 K to 1100 K (see Ref. 6 for experimental details). With this method, the p_{O_2} -dependent defect equilibria at the LAO/STO-interface can be studied in well-defined thermodynamical equilibrium conditions.

The LAO/STO-interface has been achieved by a standard pulsed laser deposition (PLD) of 8 unit cells (uc) LAO on a TiO₂-terminated STO single crystal (sc) substrate ($T = 850^\circ\text{C}$, $p_{\text{O}_2} = 2 \times 10^{-3} \text{ mbar}$).¹¹ Additionally, (La,Sr)(Al,Ta)O₃ (LSAT) has been used as an alternative substrate material for the epitaxial PLD-growth of 10 uc STO ($T = 850^\circ\text{C}$, $p_{\text{O}_2} = 0.1 \text{ mbar}$) and 10 uc LAO ($T = 850^\circ\text{C}$ and $p_{\text{O}_2} = 3 \times 10^{-5} \text{ mbar}$).¹⁷ In the following, these two heterostructures will be denominated HS1 (LAO/STO) and HS2 (LAO/STO/LSAT), respectively. A lower deposition pressure was used for the sample grown on LSAT in order to achieve a low temperature conductance and a room temperature sheet carrier density ($n_s \approx 1 \times 10^{14} \text{ cm}^{-2}$) similar to the ones measured in the HS1 sample.¹⁷ For the HTEC measurements, a STO sc, a LSAT sc (both 0.5 mm thick), and a 10 uc thick STO film on LSAT (STO/LSAT) grown at similar conditions as for HS2 were investigated as reference samples. The HTEC characteristics of HS1 and HS2 are then discussed as the sum of the LAO/STO-interface contribution and the corresponding substrate contribution.

Fig. 1(a) shows the HTEC characteristic of the single crystalline substrates, STO and LSAT, plotted on double logarithmic scales. As a result of oxygen exchange, STO shows the characteristic V-shaped curve with enhanced n -type and p -type conductance in reducing and oxidizing atmospheres, respectively.^{6,16,18} The LSAT sc shows a similar p -type behavior in oxidizing conditions, while a negligible increase of the conductance is observed in the reducing regime. In general, LSAT exhibits a significantly lower conductance than STO over the entire investigated p_{O_2} -range. Thus, LSAT is expected to substantially diminish the substrate contribution in the HTEC measurements compared to STO.

Fig. 1(b) shows the HTEC characteristic of HS1 (G_{HS1} , filled symbols) in comparison to the STO sc (G_{STO} , open symbols). Both characteristics deviate significantly for intermediate p_{O_2} due to the additional, temperature- and p_{O_2} -independent conductance contribution of the metallic LAO/

^{a)}Electronic mail: f.gunkel@fz-juelich.de.

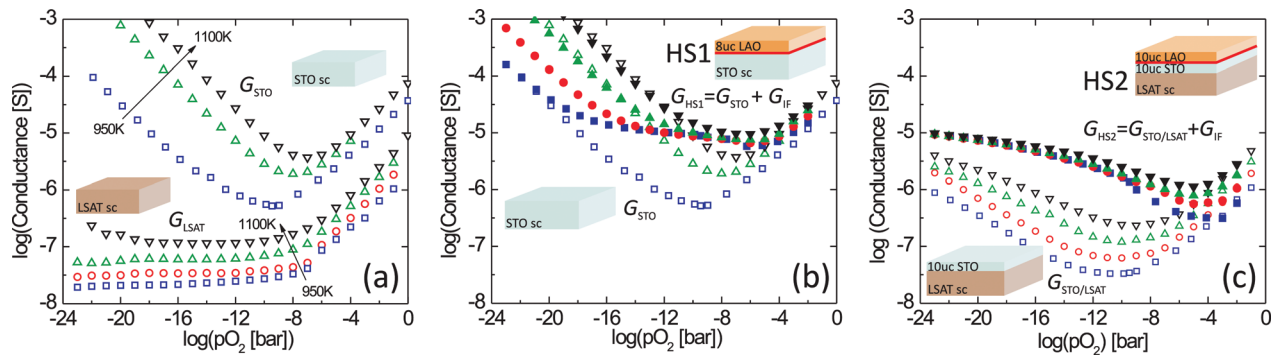


FIG. 1. (Color) HTEC characteristics of (a) a STO and LSAT single crystal, (b) the standard LAO/STO-heterostructure (HS1, filled symbols) in comparison to the STO substrate (open symbols), and (c) the LAO/STO/LSAT-heterostructure (HS2, filled symbols) in comparison to the STO/LSAT-stack (open symbols) at various temperatures: 950 K (■), 1000 K (●), 1050 K (▲), and 1100 K (▼).

STO-interface (G_{IF}).⁶ In the reducing regime as well as in the oxidizing regime, G_{IF} is concealed by the dominating substrate contribution G_{STO} .

The HTEC characteristics of HS2 (G_{HS2} , filled symbols) and the STO thin film on LSAT ($G_{STO/LSAT}$, open symbols) are illustrated in Fig. 1(c). Compared to the bare LSAT sc (Fig. 1(a)), the HTEC characteristic of the STO/LSAT-sample shows an additional conductance upturn due to the STO-layer in strongly reducing atmosphere. Accordingly, the STO/LSAT-data have to be taken as a reference for HS2. A clear impact of the metallic LAO/STO-interface is observed below 10^{-4} bar where HS2 shows a significantly enhanced conductance compared to the STO/LSAT-stack. For reducing conditions, the LAO/STO-interface of HS2 exhibits a plateau-like conductance behavior with very weak dependence on temperature and pO_2 which resembles the behavior of the standard LAO/STO-interface in HS1. Approaching oxidizing conditions ($pO_2 > 10^{-12}$ bar), however, a deviation from the constant behavior is observed. This pO_2 -dependence of the interface conductance will be further discussed.

For the pO_2 -regions, in which the heterostructures exhibit a significantly higher conductance than the corresponding reference samples, the conductance contribution of the LAO/STO-interface G_{IF} can be calculated as $(G_{HS1} - G_{STO})$ and $(G_{HS2} - G_{STO/LSAT})$, respectively. The corresponding sheet carrier density $n_s = G_{IF}/e\mu_n$ can then be determined by a proper estimation of the electron mobility μ_n . For the investigated temperature range above 900 K, μ_n is limited by phonon scattering resulting in a power law type temperature dependence. Reference data for μ_n , obtained from a 5at. % La-doped STO sc, showed a good agreement with the temperature dependence reported in Ref. 16 ($\mu_n = 3.95 \times 10^4 \times T[K]^{-1.62} \text{ cm}^2/\text{Vs}$). Therefore, this value was applied to calculate the interfacial sheet carrier density of HS1 and HS2. These results are shown in Fig. 2.

In the pO_2 -independent plateau region, n_s approaches a value of $1 \times 10^{14} \text{ cm}^{-2}$ for both samples, which is consistent with the carrier densities obtained from Hall measurements¹⁷ as well as from spectroscopic investigations.¹⁹ For oxidizing conditions, HS2 shows a steep decrease of n_s with a slope of approximately $(-1/4)$ in the double logarithmic plot. In this region, the temperature dependence of n_s follows an Arrhenius-type law with an activation energy (E_A) of about 1 eV (see inset of Fig. 2). HS1 shows a similar tendency of a decreasing n_s with increasing pO_2 above 10^{-8} bar. Due to

the large STO substrate contribution at oxidizing conditions, however, this tendency is concealed above 10^{-4} bar.

The measured HTEC characteristics of the LAO/STO-interfaces resemble the HTEC behavior of donor-doped STO (Ref. 16) and can, therefore, be discussed within the corresponding defect chemistry model. Donor-doped STO shows a pO_2 -independent region in its HTEC characteristic for which the charge neutrality condition $n = [D^\bullet]$ is valid (full electronic compensation). Here, n denotes the electron concentration and $[D^\bullet]$ the concentration of ionized extrinsic donors. In this plateau region, the concentration of mobile oxygen vacancies $[V_O^{\bullet\bullet}]$ is much smaller than $[D^\bullet]$,¹⁶ so that n is unaffected by oxidation or reduction reactions. According to this model, the plateau-like region in the HTEC characteristics of HS1 and HS2, observed for reducing conditions, indicates the presence of donor dopants at the LAO/STO-interface provided for example by cation-intermixing.

In order to maintain charge neutrality, a decrease of n below the donor level $[D^\bullet]$ requires the formation of additional compensating defects which carry a negative net charge. Predominately, Sr-vacancies (V_{Sr}'') are considered as acceptor-type cationic defects in STO. These can be reversibly created and annihilated¹⁶ according to the reaction

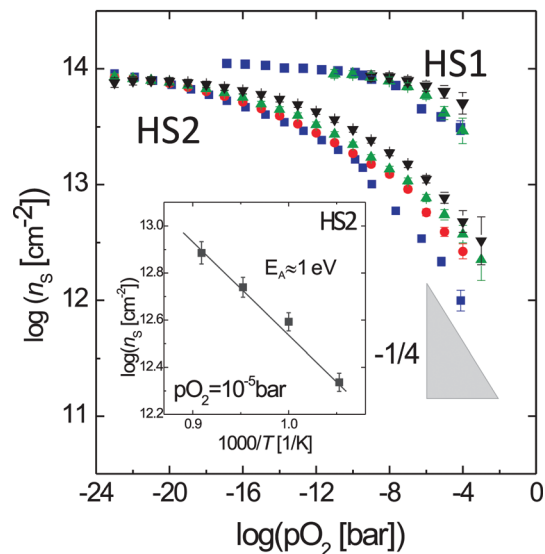
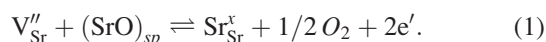


FIG. 2. (Color) The sheet carrier density n_s at the LAO/STO-interface as a function of pO_2 at various temperatures (950 K (■), 1000 K (●), 1050 K (▲), and 1100 K (▼)). HS1 corresponds to LAO/STO, HS2 to LAO/STO/LSAT. Inset: Arrhenius-plot of n_s at $pO_2 = 10^{-5}$ bar for HS2.



Here, $(\text{SrO})_{\text{sp}}$ denotes a Sr-rich secondary phase and e' a free electron. The corresponding law of mass action leads to the expression

$$\frac{p\text{O}_2^{1/2} \cdot n^2}{[V''_{\text{Sr}}]} \propto \exp\left(-\frac{H_V}{k_B T}\right), \quad (2)$$

where H_V is the reaction enthalpy. For a given temperature, it follows from Eq. (2), that $[V''_{\text{Sr}}]$ increases with increasing $p\text{O}_2$. Hence, an increasing fraction of donors is compensated by Sr-vacancies when the ambient $p\text{O}_2$ is increased. In case of a full ionic compensation of the extrinsic donors ($[V''_{\text{Sr}}] = 1/2[D^{\bullet}] = \text{const.}$), n becomes proportional to $p\text{O}_2^{-1/4}$. The characteristic slope of $(-1/4)$, which results on double logarithmic scales, is also observed for HS2. This indicates that the decrease of n_S at the LAO/STO-interface for oxidizing conditions originates from a self-compensation mechanism caused by Sr-vacancies. It follows for HS2, that $[V''_{\text{Sr}}]$ has to reach a value of about $1.3 \times 10^{20} \text{ cm}^{-3}$ within the 10 uc thick STO-layer in order to compensate for an interfacial donor concentration of $1 \times 10^{14} \text{ cm}^{-2}$. The reaction enthalpy H_V can be calculated from E_A , which was determined for HS2 at oxidizing conditions, via $H_V = 2E_A \approx 2 \text{ eV}$. This value obtained for the LAO/STO-interface differs significantly from the value for bulk STO (3.6 eV).¹⁶ Although a clear $(-1/4)$ -behavior cannot be observed for HS1, the evolving decrease of n_S above 10^{-8} bar suggests that a similar charge compensation effect is present at the interface of the standard LAO/STO-heterostructure. Compared to sample HS2, however, the decrease of n_S is shifted towards higher $p\text{O}_2$ -values indicating an effect of the particular STO-environment in a single crystal (HS1) and a (more defective)²⁰ thin film (HS2), respectively.

In conclusion, the *in-situ* study of the HTEC of LAO/STO-heterostructures emphasizes the importance of crystal disorder for the electronic properties of the LAO/STO-interface. The observed $p\text{O}_2$ - and temperature-independence of the sheet electron density for reducing conditions supports the idea of a donor-type conduction mechanism at the LAO/STO-interface such as provided by cation-intermixing. Furthermore, the decrease of n_S in oxidizing conditions indicates a complex charge compensation mechanism in the vicinity of the interface which involves the formation of Sr-vacancies at high oxygen partial pressures. This implies that oxygen annealing after the growth of LAO/STO-heterostructures,

which is commonly thought to merely remove oxygen vacancies from the STO substrate, can also result in an increased cation vacancy concentration at the interface. These additional defects can reduce the electron density and, moreover, can act as scatter centers at low temperatures.

As pivotal result of this study, it has been shown that in the vicinity of the LAO/STO-interface exchange reactions in the cation sublattice, i.e., formation and annihilation of strontium vacancies take place at typical growth temperatures and have to be considered in the discussion of the LAO/STO-interface.

¹A. Ohtomo and H. Y. Hwang, *Nature* **427**, 423 (2004).

²S. A. Pauli and P. R. Willmott, *J. Phys. Condens. Matter* **20**, 264012 (2008).

³M. Huijben, A. Brinkman, G. Koster, G. Rijnders, H. Hilgenkamp, and D. H. A. Blank, *Adv. Mater.* **21**, 1665 (2009).

⁴J. Mannhart, D. H. A. Blank, H. Y. Hwang, A. J. Millis, and J. M. Triscone, *MRS Bull.* **33**, 1027 (2008).

⁵N. Nakagawa, H. Hwang, and D. Muller, *Nature Mater.* **5**, 204 (2006).

⁶F. Gunkel, S. Hoffmann-Eifert, R. Dittmann, S. B. Mi, C. L. Jia, P. Meuffels, and R. Waser, *Appl. Phys. Lett.* **97**, 012103 (2010).

⁷A. Kalabukhov, Y. A. Boikov, I. T. Serenkov, V. I. Sakharov, J. Borjesson, N. Ljustina, E. Olsson, D. Winkler, and T. Claeson, *EPL* **93**, 37001 (2011).

⁸P. R. Willmott, S. A. Pauli, R. Herger, C. M. Schlepütz, D. Martoccia, B. D. Patterson, B. Delley, R. Clarke, D. Kumah, C. Cionca *et al.*, *Phys. Rev. Lett.* **99**, 155502 (2007).

⁹L. Qiao, T. C. Droubay, V. Shutthanandan, Z. Zhu, P. V. Sushko, and S. A. Chambers, *J. Phys. Condens. Matter* **22**, 312201 (2010).

¹⁰S. A. Chambers, M. H. Engelhard, V. Shutthanandan, Z. Zhu, T. C. Droubay, L. Qiao, P. V. Sushko, T. Feng, H. D. Lee, T. Gustafsson *et al.*, *Surf. Sci. Rep.* **65**, 317 (2010).

¹¹A. Brinkman, M. Huijben, M. van Zalk, J. Huijben, U. Zeitler, J. C. Maan, W. G. van der Wiel, G. Rijnders, D. H. A. Blank, and H. Hilgenkamp, *Nature Mater.* **6**, 493 (2007).

¹²C. Cancellieri, N. Reyren, S. Gariglio, A. D. Caviglia, A. Fete, and J. M. Triscone, *EPL* **91**, 17004 (2010).

¹³W. Siemons, G. Koster, H. Yamamoto, W. A. Harrison, G. Lucovsky, T. H. Geballe, D. H. A. Blank, and M. R. Beasley, *Phys. Rev. Lett.* **98**, 196802 (2007).

¹⁴M. Basletic, J. L. Maurice, C. Carretero, G. Herranz, O. Copie, M. Bibes, E. Jacquet, K. Bouzehouane, S. Fusil, and A. Barthelémy, *Nature Mater.* **7**, 621 (2008).

¹⁵A. Kalabukhov, R. Gunnarsson, J. Borjesson, E. Olsson, T. Claeson, and D. Winkler, *Phys. Rev. B* **75**, 121404(R) (2007).

¹⁶R. Moos and K. H. Haerdtl, *J. Am. Ceram. Soc.* **80**, 2549 (1997).

¹⁷P. Brinks, W. Siemons, J. E. Kleibeuker, G. Koster, G. Rijnders, and M. Huijben, *Appl. Phys. Lett.* **98**, 242904 (2011).

¹⁸D. M. Smyth, *The Defect Chemistry of Metal Oxides* (Oxford University Press, New York, 2000).

¹⁹G. Berner, S. Glawion, J. Walde, F. Pfaff, H. Hollmark, L. C. Duda, S. Paetel, C. Richter, J. Mannhart, M. Sing, and R. Claessen, *Phys. Rev. B* **82**, 241405 (2010).

²⁰D. J. Keeble, S. Wicklein, R. Dittmann, L. Ravelli, R. A. Mackie, and W. Egger, *Phys. Rev. Lett.* **105**, 226102 (2010).